Introducing a New Serpentine Configuration of Gas Channels to Enhance the Performance and Reduce the Water Flooding in the PEMFC

Ashrafi, Hojjat•; Pourmahmoud, Nader; Mirzaee, Iraj
Mechanical Engineering Department, Urmia University, Urmia, I.R. IRAN

Ahmadi, Nima*[+]
Department of Mechanical Engineering, Technical and Vocational University (TVU), Tehran, I.R. IRAN

ABSTRACT: *Proton-exchange membrane fuel cells consume hydrogen and air and have high efficiency and power density. The present study three-dimensionally investigates the performance of PEMFCs with different geometries under different operating conditions. The computational fluid dynamics approach was adopted to solve the governing equations. In CFD, the finite volume method is employed to discretize and solve equations. A serpentine gas injection channel and a parallel gas injection channel of the same size were examined. The proposed approach was validated by simulating the base model at 0.6 V and three reference current densities. The present work primarily sought to improve the performance of PEMFCs. Also, the concentration diagram indicated that the water concentration rose on the cathodic side, implying reasonable water transfer management was reasonable. Moreover, the oxygen concentration declined on the cathodic side. The serpentine model was found to have a higher current density and output power than the parallel model. Liquid water production was lower in the serpentine model than in the parallel model. This prevented immersion and fuel cell interruption. Water accumulation in the middle of the PEMFC with the parallel channel hindered uniform temperature and current density distributions. The parallel model underwent a lower pressure drop than the serpentine model. Therefore, lower power was required to pump the gases through the parallel channel. A rise in the reference current density reduced liquid water production and overpotential and improved the current density distribution and temperature distribution in both serpentine and parallel models.*

KEYWORDS: *Proton-exchange membrane fuel cell; Operating conditions; Reference current density; Gas channel geometry; Performance improvements.*

***** *To whom correspondence should be addressed.*
+ *E-mail: Nima.Ahmadi.Eng@gmail.com*
• *Other Address: Department of Mechanical Engineering, Technical and Vocational University (TVU), Tehran, I.R. IRAN*
1021-9986/2023/1/192-207 16/$/6.06

INTRODUCTION

Energy shortage and environmental pollution imposed by different industries continue to become more serious due to technological advances. Therefore, researchers have been promoting the development of new energy technologies worldwide [1, 2]. Fuel cells have a quiet operation, generate renewable energy, and produce no pollution. They are the most ideal newly developed energy resource [3, 4]. Fuel cells convert chemical energy in fuel into electricity. In light of advantages such as high power density, safety, and a simple structure, fuel cells are widely used in many applications, such as appliances and vehicles. Many parameters, e.g., humidity, gas injection channel geometry, temperature, pressure, and membrane structure, influence the performance of a fuel cell. Therefore, it is essential to investigate and improve fuel cell performance [5, 6]. The poor adjustment of operating parameters may have a serious adverse impact on the efficiency of a fuel cell and even accelerate its efficiency decline. Therefore, it is crucial to study the effects of operating parameters on the performance of fuel cells [7]. Many researchers have reported useful results in recent years. *Wang et al.* [8] carried out tests on different operating parameters to explore their impacts on fuel cell performance. *Santarelli et al.* [9] investigated the behavior of a proton-exchange membrane fuel cell (PEMFC) using operating parameters, such as humidity, pressure, and temperature. They concluded that a rise in pressure could improve PEMFC performance. *Yang et al.* [10] studied the impacts of operating parameters on a fuel cell with a close-end anode. *Kim et al.* [11] evaluated the effects of pressure under different conditions. They found that the output voltage increased as the operating pressure increased. *Kadjo et al.* [12] analyzed the effects of pressure and temperature on the electrical performance of a fuel cell. *Kahveci et al.* [13] found that a rise in the operating pressure enhanced fuel cell performance. The performance of the fuel cell began to decline when the temperature exceeded a threshold, and a reduction in the relative humidity of the cathode could help improve fuel cell performance. *Zeroual et al.* [14] studied the effects of pressure on fuel cell performance. The results indicated that a rise in pressure improved water discharge and increased the reaction rate. Through numerical simulations, *Kim et al*. [15] found that the input humidity of the cathode and anode had significant effects on the performance of a fuel cell, and excessive humidity in the cathode would induce floods in the cathodic catalyst layer. *Zhang et al.* [16] explored the effects of relative humidity, air stoichiometry, and backpressure on PEMFCs. It was found that the overall performance and current distribution uniformity improved as relative humidity increased. *Chavan et al.* [17] analyzed the impacts of hydrogen flow, hydrogen humidity, and partial hydrogen pressure on the performance of fuel cells by controlling input parameters. *Wang et al.* [18] recommended efficient cathode humidity reduction, anode stoichiometry enhancement, and equal anode and cathode input pressure rises to improve fuel cell performance. *Guvelioglu et al.* [19] simulated a fuel cell using MATLAB and concluded that a rise in the hydrogen rate and a decline in the airflow with 100% humidity improved fuel cell performance. *Gomez et al.* [20] humidified the input gas of the fuel cell to maintain better water management. *Boulon et al.* [21] prevented immersion in the fuel cell or a dried membrane by controlling the humidity of input air. *Wasterlain et al.* [22] found that a higher operating temperature and airflow velocity could increase the output voltage; however, membrane water deficiency was likely to occur. *Ahmadi et al.* [23-25] evaluated fuel cell performance and species distributions by investigating different parameters. Apart from the effects of operating parameters, the geometry of the gas injection channel has a significant effect on the efficiency improvement of a fuel cell. *Ahmed et al*. [26] developed a numerical model to evaluate the performance of PEMFCs at high current densities for different gas injection channel geometries. It was found that the rectangular channel section generated higher voltage, while the trapezoidal channel had a more uniform distribution. *Jabbary et al.* [27] investigated the effects of rhomboid channels on the performance of PEMFCs. Several studies have been conducted on the effects of serpentine channels on PEMFC performance [28-30]. *Ozdemir et al.* [31] studied U-shaped, Z-shaped, and serpentine gas injection channels. *Samanipour et al.* [32] examined cylindrical fuel cells and concluded that the cylindrical model outperformed the base model. *Mohammedi et al.* [33] studied the effects of density, pressure drop, and power in three-dimensional trapezoidal models. *Sadeghi et al.* [34] numerically simulated different three-dimensional PEMFCs, including a sinusoidal model. *Sheikhmohammadi et al.* [35] proposed new designs of

Table 1: Geometric characteristics of the base model [28].

Parameters	Value
Channel height	1×10^{-3} m
Channel width	0.8×10^{-3} m
Channel area	8×10^{-7} m^2
Effective land area	11×10^{-4} m^2
CL thickness	0.03×10^{-4} m
GDL thickness	2.5×10^{-4} m
Membrane thickness	0.5×10^{-4} m

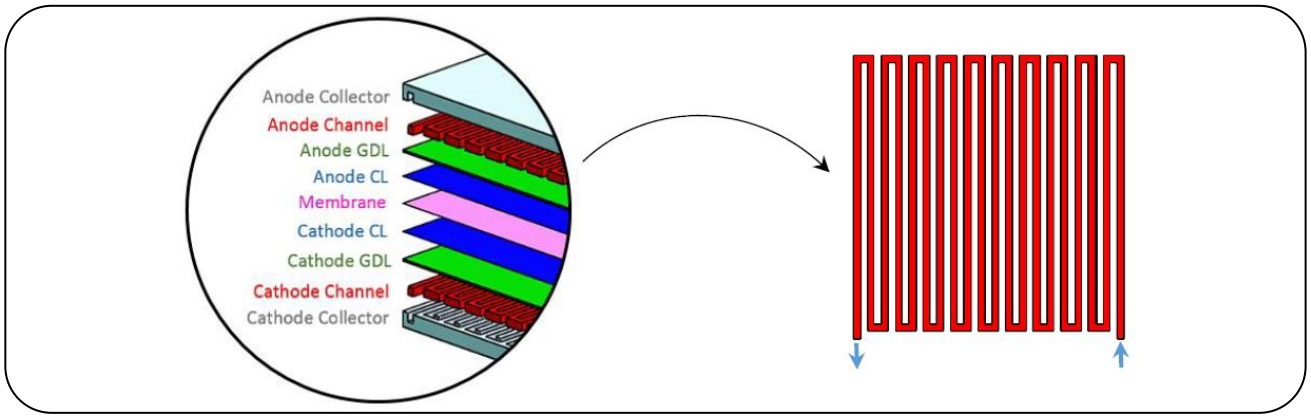

Fig. 1: PEMFC base model.

the gas channel and investigated PEMFC performance.

As the designing of the gas channels is one of the key parameters in the output performance of the PEMFC, It is necessary to improve the performance of fuel cells based on operating conditions and gas channel geometry. Therefore, the present study numerically compares PEMFCs with a parallel and a serpentine flow field, investigating the impacts of different operating parameters on PEMFC performance. In the present work, the new design of the PEMFC is introduced. The new design that is introduced in this study has a lesser pressure drop compared with the base model. This fact leads to less power consumption to pump the species into the reaction area.

THEORETICAL SECTION

Mathematical model

A three-dimensional serpentine model was selected as the base model, as shown in Fig. 1. Table 1 reports the geometric description of the base model.

Model assumptions

(1) The reactants are ideal, and the ideal gas law holds.

(2) The fluid flow is incompressible and the model is three-dimensional.

(3) The fluctuations induced by air and hydrogen transfer are neglected.

(4) The fuel cell operates in a steady state.

(5) The fuel cell has a constant temperature, neglecting the gradient effect.

(6) The membrane is completely impermeable to the reactants.

(7) The porous medium of the diffusion layer, catalyst layer, and proto-exchange layer is isotropic.

Governing equations

Table 2 shows the governing equations of a PEMFC, including the continuity, momentum, species, and potential equations.

In the continuity equation, ρ denotes the mixture density, while ε is the effective porosity of the porous layer. Also, μ is the viscosity of the gas mixture in the motion equation, and S_u is the source term of the momentum equation. Further details on the governing equations are provided in earlier works [2, 7, 25, 36]. As these equations have the source terms in the different layers of the PEMFC, and the source term of the equation

Table 2: Governing equations.

Term	Equation
continuity	$(\nabla.\rho u) = 0$
momentum	$\frac{1}{(\varepsilon^{eff})^2}\nabla.(\rho uu) = -\nabla P + \nabla.(\mu\nabla u) + S_u$
species	$\nabla.(uC_k) = \nabla.\left(D_k^{eff}\nabla C_k\right) + S_k$
potential	$\nabla.\left(K_e^{eff}\nabla\Phi_e\right) + S_\Phi = 0$

Table 3: Source/Sink term for conservation equations [24].

	Momentum	species	charge
Flow channels	$S_u = 0$	$S_K = 0$	$S_\Phi = 0$
Bipolar plates	$S_u = -\frac{\mu}{K}u$	$S_K = 0$	$S_\Phi = 0$
GDLs	$S_u = -\frac{\mu}{K}u$	$S_K = 0$	$S_\Phi = 0$
Catalyst layers	$S_u = 0$	$S_K = -\nabla\left(\frac{n_d}{F}I\right) - \frac{S_K J}{nF}$	$S_\Phi = j$
Membrane	$S_u = 0$	$S_K = -\nabla\cdot\left(\frac{n_d}{F}I\right)$	$S_\Phi = 0$

Table 4. Boundary conditions.

Location in fuel cell geometry	Assumption of the boundary condition
Anode gas channel inlet	$u = u_{in}$, $T = T_{in}$, $v = 0$, $C_{H_2} = C^a{}_{H_2,in}$, $C_{H_2O} = C^a{}_{H_2o,in}$
Cathode gas channel inlet	$u = u_{in}$, $T = T_{in}$, $v = 0$, $C_{o_2} = C^c{}_{o_2,in}$, $C_{N_2} = C^c{}_{N_2,in}$
Anode and cathode gas channel outlet	$\frac{\partial u}{\partial x} = \frac{\partial v}{\partial x} = \frac{\partial w}{\partial z} = \frac{\partial T}{\partial x} = 0$
GDL and gas channels interface	$\frac{\partial u}{\partial y}_{y=h_1^-} = \varepsilon_{eff,GDL}\frac{\partial u}{\partial y}_{y=h_1^+}$, $\frac{\partial v}{\partial y}_{y=h_1^-} = \varepsilon_{eff,GDL}\frac{\partial v}{\partial y}_{y=h_1^+}$, $\frac{\partial w}{\partial y}_{y=h_1^-} = \varepsilon_{eff,GDL}\frac{\partial w}{\partial y}_{y=h_1^+}$
GDL and CL interface	$\varepsilon_{eff,GDL}\frac{\partial u}{\partial y}_{y=h_2^-} = \varepsilon_{eff,CL}\frac{\partial u}{\partial y}_{y=h_2^+}$, $\varepsilon_{eff,GDL}\frac{\partial v}{\partial y}_{y=h_2^-} = \varepsilon_{eff,CL}\frac{\partial v}{\partial y}_{y=h_2^+}$, $\varepsilon_{eff,GDL}\frac{\partial w}{\partial y}_{y=h_2^-} = \varepsilon_{eff,CL}\frac{\partial w}{\partial y}_{y=h_2^+}$
Membrane and CTL interface	$u = v = w = C_i = 0$
Top surface of gas channel	$u = v = w = C_i = 0$, $T_{surface} = 353K$
Bottum surface of gas channel	$u = w = 0$, $T_{surface} = T_{wall}$
Top surface of anode bipolar	$\phi_{sol} = 0$, $\frac{\partial\phi_{mem}}{\partial y} = 0$
Top surface of cathode bipolar	$\phi_{sol} = V_{cell}$, $\frac{\partial\phi_{mem}}{\partial y} = 0$
External surfaces	$\frac{\partial\phi_{mem}}{\partial x} = 0$, $\frac{\partial\phi_{mem}}{\partial z} = 0$, $\frac{\partial\phi_{sol}}{\partial x} = 0$, $\frac{\partial\phi_{sol}}{\partial z} = 0$

for the layers are listed in Table 3.

The boundary conditions of the PEMFC for all regions are presented and listed in Table 4.

Solution

Computational Fluid Dynamics (CFD) was adopted to solve the governing equations. The equations are discretized).

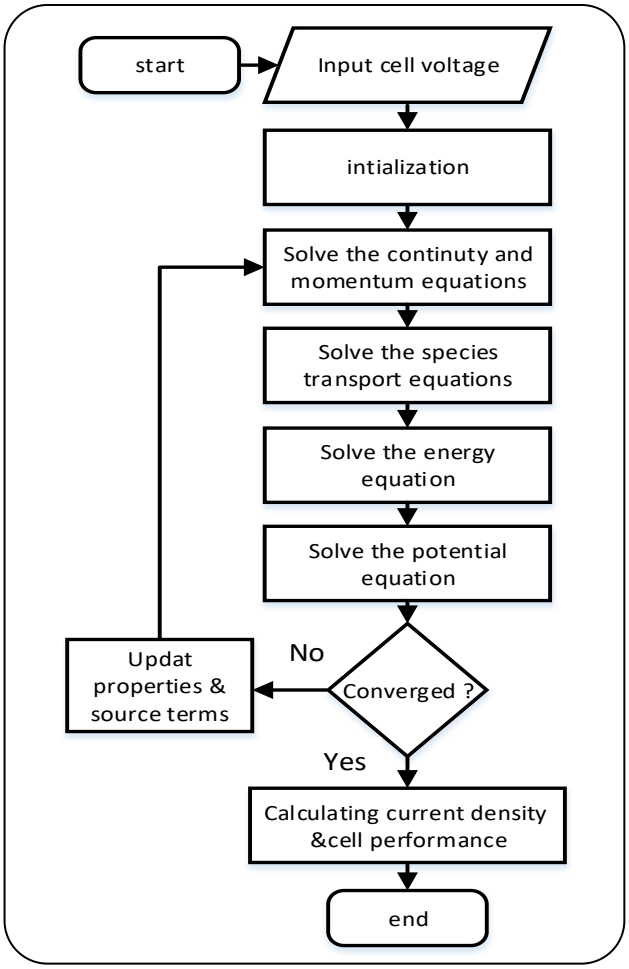

Fig. 2: Solution algorithm.

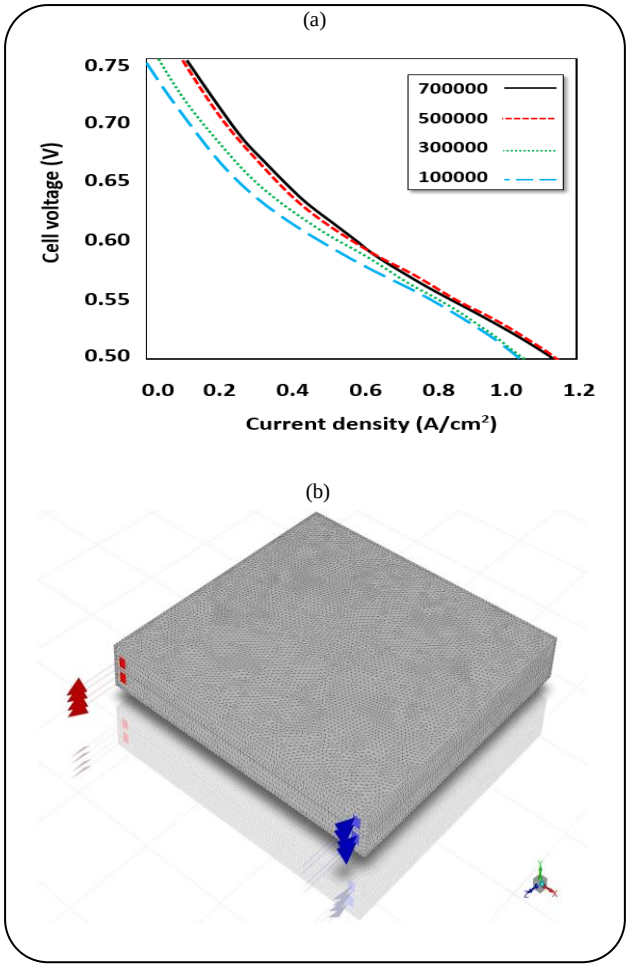

Fig. 3. Mesh independence check results (a), the 3D grid of the model (b).

and solved using the Finite Volume Method (FVM The SIMPLE algorithm was employed to couple pressure and velocity [37]. The convergence criterion was defined to be met when the solution residuals of the equations reduced below 10^{-3} in the continuity equation, 10^{-6} in the energy equation, and 10^{-10} in the potential equation and when the output current remained unchanged for at least four iterations [38]. Fig. 2 depicts the solution algorithm.

To find the optimal mesh size, a coarse grid was initially tested. It was found that the use of finer elements changed the computation output. A rise in the number of elements to 700,000 led to no significant change in the output. Therefore, a total of 500,000 elements were employed to save computation time. Fig.3a indicates the grid independence check results. The three-dimensional grid of the studied domain is presented in Fig. 3b. Also, in this figure the domain and the shape of the base model is clear.

Table 5 reports the operating parameters. They were selected based on the model proposed by *Jeon et al.* [28]. This study utilized a computer with a 16-core CPU, 24GB RAM, and a 100GB HDD. Each simulation round was completed in nearly 3 hours.

RESULTS AND DISCUSSION

The simulation results are compared to *Jeon et al.* [28]. According to Fig. 4, the numerical results were in good agreement with F. This demonstrates the validity of the proposed model. The present study numerically and comparatively analyzed a parallel flow field and a serpentine flow field (the base model), as shown in Fig. 5.

The effects of the reference current density were explored for both models. In general, the same reaction area, model assumptions, and boundary conditions (except for the anode

Table 5: Parameters and performance conditions [28].

Parameter	Value
Mass fraction of H_2 at anode inlet	0.115
Mass fraction of H_2O at anode inlet	0.885
Mass fraction of O_2 at cathode inlet	0.183
Mass fraction of H_2O at cathode inlet	0.215
Relative humidity	1
Open circuit voltage (V)	0.96
Pressure (kPa)	101
Temperature (°C)	80

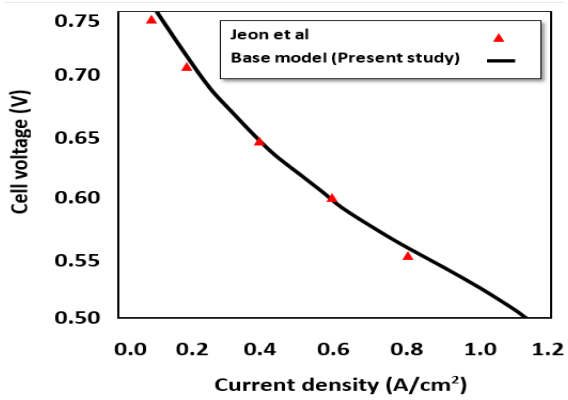

Fig. 4: Polarization curve of model validation.

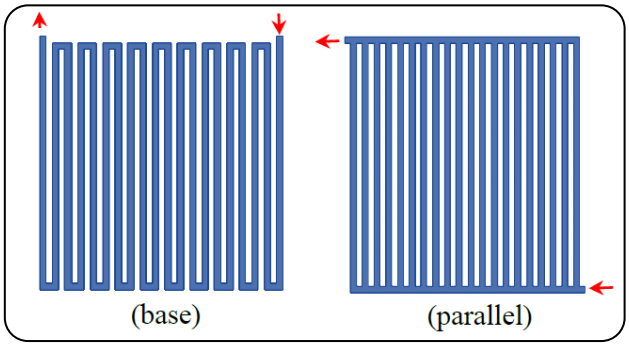

Fig. 5: Base model and parallel model.

and cathode inflow rates) were applied to find the optimal model.

Table 6 represents the inflow rates at different reference current densities.

Fig. 6 compares the polarization curves of the models. The numerical results indicate that the serpentine model had a higher current density and output power than the parallel model, as shown in Figs. 7 and 8.

Table 6: Inflow rates at different reference current densities.

Parameter	Value		
I_{ref} (A/m$^{2)}$)	6000	12000	18000
Mass flowrate at anode inlet (kg/s)	7.13265×10^{-7}	1.42653×10^{-6}	2.13979×10^{-6}
Mass flowrate at cathode inlet (kg/s)	6.1064×10^{-6}	1.22128×10^{-5}	1.83192×10^{-5}

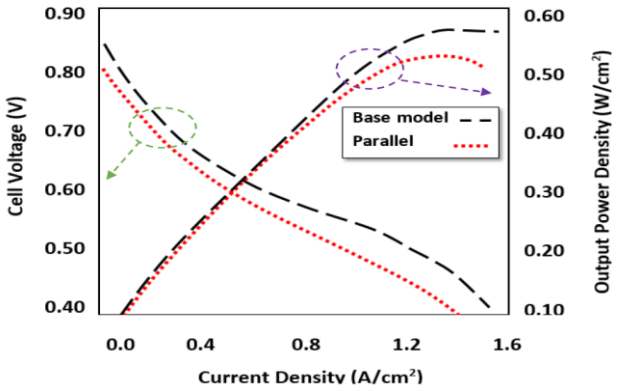

Fig. 6: Polarization curves of different models.

As can be seen in Figs. 7 and 8, the base model produces more current density and output power density than the parallel model in the same cell voltage and the same operating condition. The maximum current density is 1.51 A/cm^2 at 0.4 V and the lowest is 0.03 A/cm^2 at 0.8 V.

Figs. 9-11 illustrate the hydrogen and water mass fractions on the anodic side for both models. Hydrogen and water were found to have physically reasonable distributions along the PEMFC. The hydrogen and water mass fractions on the anodic side were observed to rise as the reference current density increased. The maximum water mass fraction on the anode side is 0.841 and the lowest is 0.789.

Figs. 12-15 illustrate the oxygen and water mass fractions on the cathodic side for both models. The water distributions on the cathodic and anodic sides should have a balanced interaction; that is when the water concentration declines along the anode due to the transfer

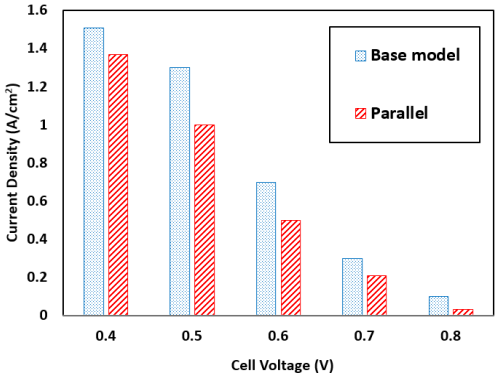

Fig. 7: Current density for different voltages.

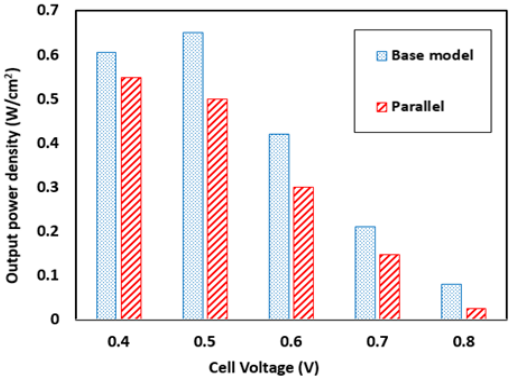

Fig. 8: Output power density for different voltages.

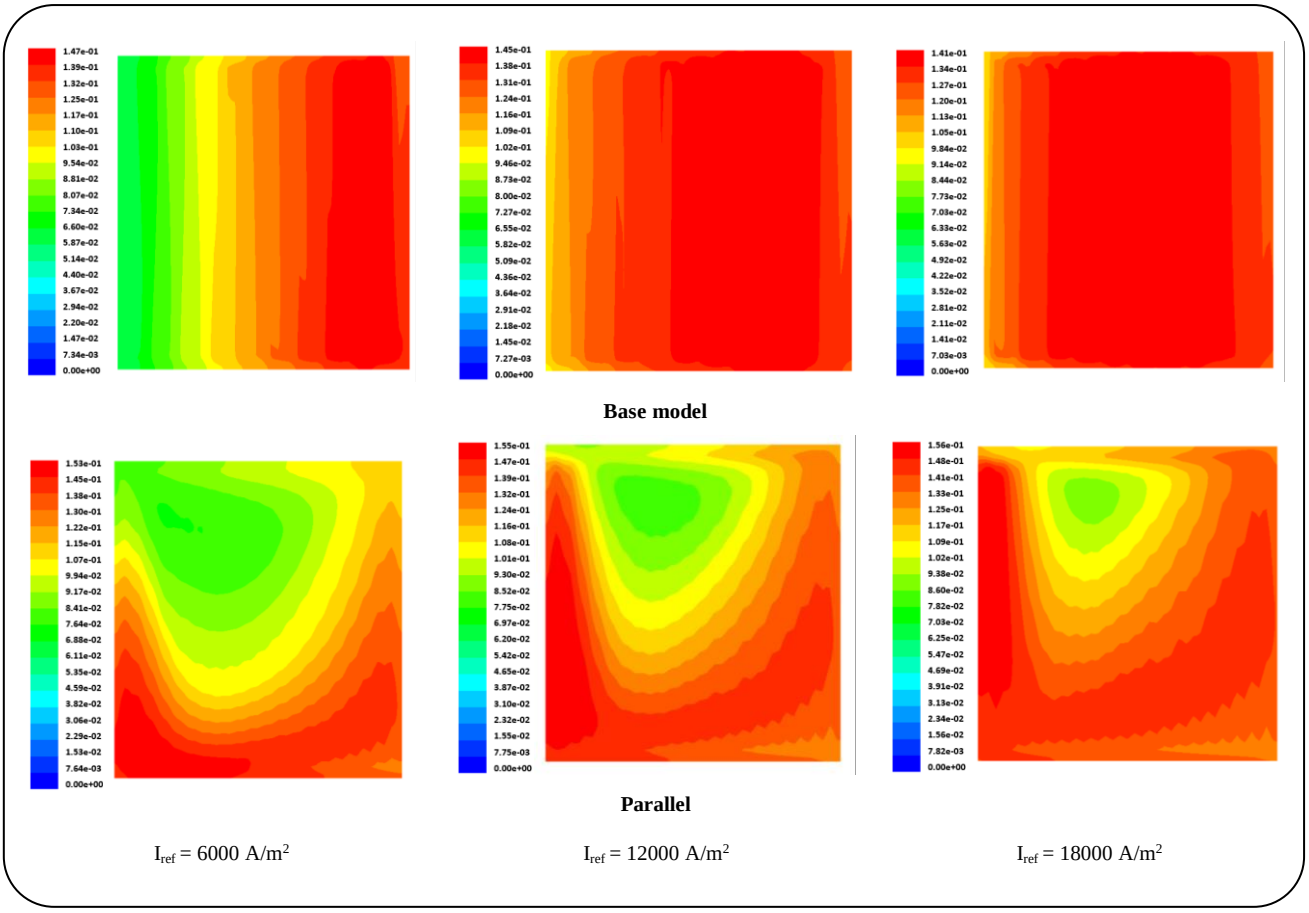

Fig. 9: Hydrogen mass fraction contours on the anode side.

of H^+ protons into the electrochemical reaction site, the water concentration on the cathodic side should rise due to the combination of molecules with oxygen, electrons, and H^+. A rise in the reference current density was observed to raise the oxygen and water mass fractions on the anodic side. The maximum water mass fraction on the cathode side is 0.355 and the lowest mass fraction of oxygen is 0.069.

The outflow rate is the most important factor in the performance evaluation of a PEMFC. Fig. 16 depicts the average current density for the models. As can be seen, the base (serpentine) model had a larger average current density at I_{ref}=18000 A/m^2 and a uniform distribution. In the parallel, however, the current density is not uniformly distributed due to water accumulation in the middle

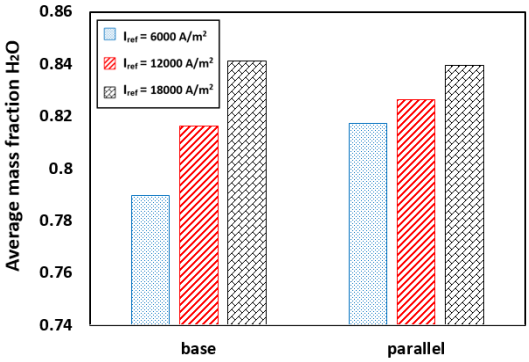

Fig. 10: Average water mass fraction on the anode side.

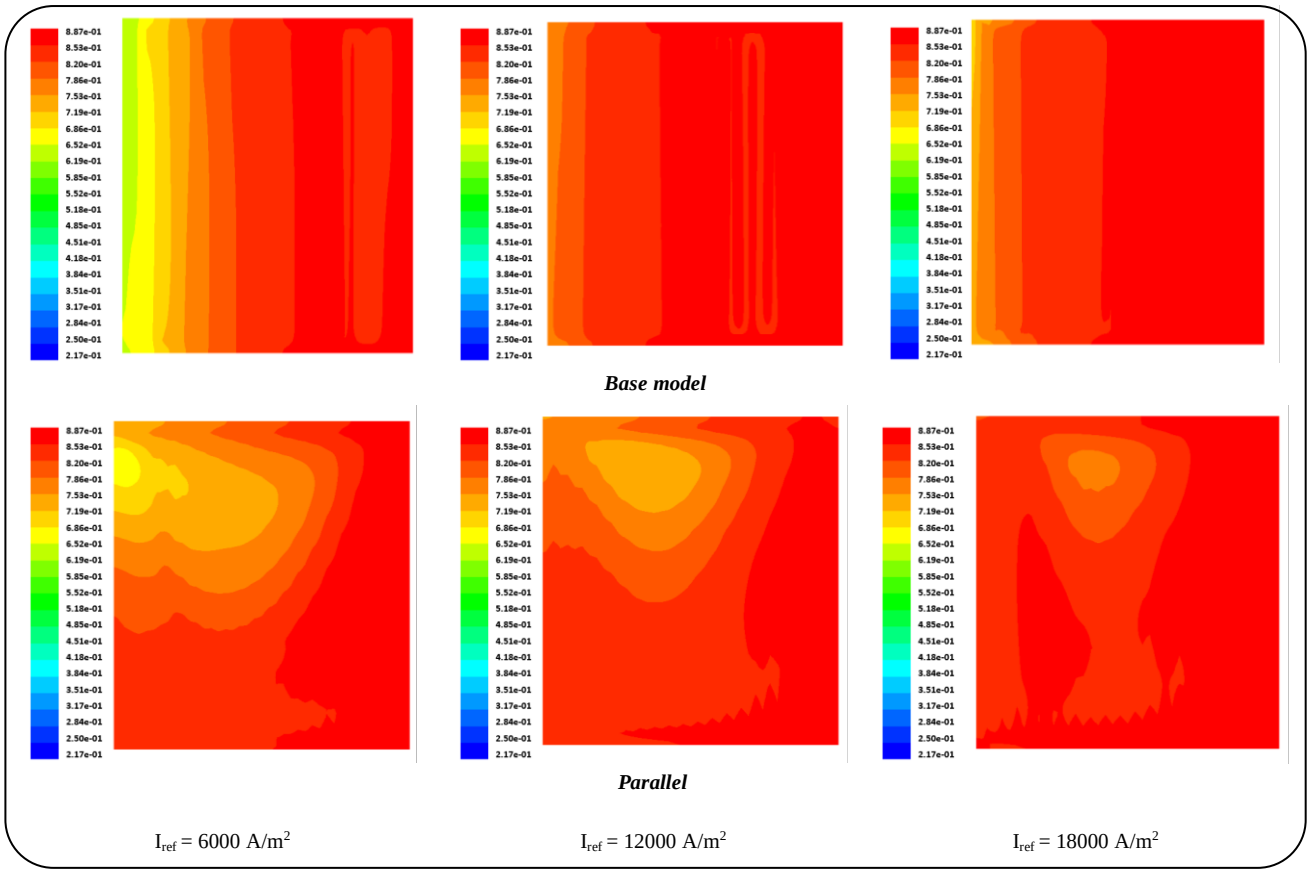

Fig. 11:Water mass fraction contours on the anode side.

of the PEMFC, particularly at I_{ref}=6000 A/m^2. Fig. 17 compares the models in the power distribution. As can be seen, power generation increased as the output current increased. The power generation of a PEMFC is calculated as $P_{fc} = I \times V \times A_{EL}$, in which I is the generated current, V is the generated voltage, and A_{EL} is the effective area of the electrode. The maximum power generation for 0.889 A/cm^2 is 5.87 W.

Pressure drop is an important challenge in a fuel cell and prevents the flow of fluids to the end of the channel at sufficient pressure. This leads to a non-uniform distribution of the current density. As can be seen in Figs. 19 and 20, the base model underwent a larger pressure drop, leading to performance deterioration. On the other hand, the parallel model experienced a lower drop in pressure along with the fuel cell. The lowest pressure drop in the parallel model for 6000 A/m^2 is 127.11 Pa.

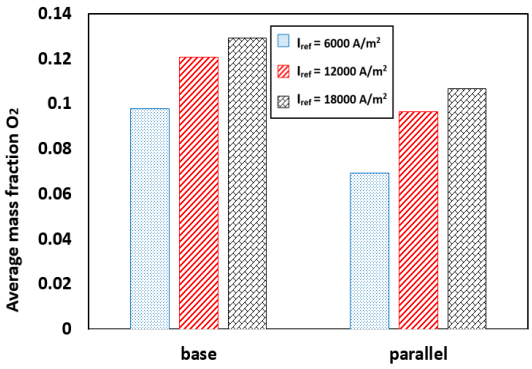

Fig. 12: Average O_2 mass fraction in the cathode side.

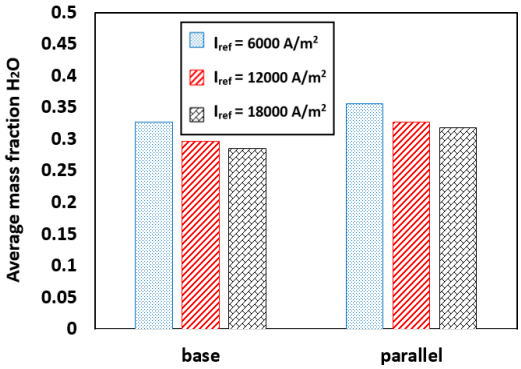

Fig. 13: Average H_2O mass fraction in the cathode side.

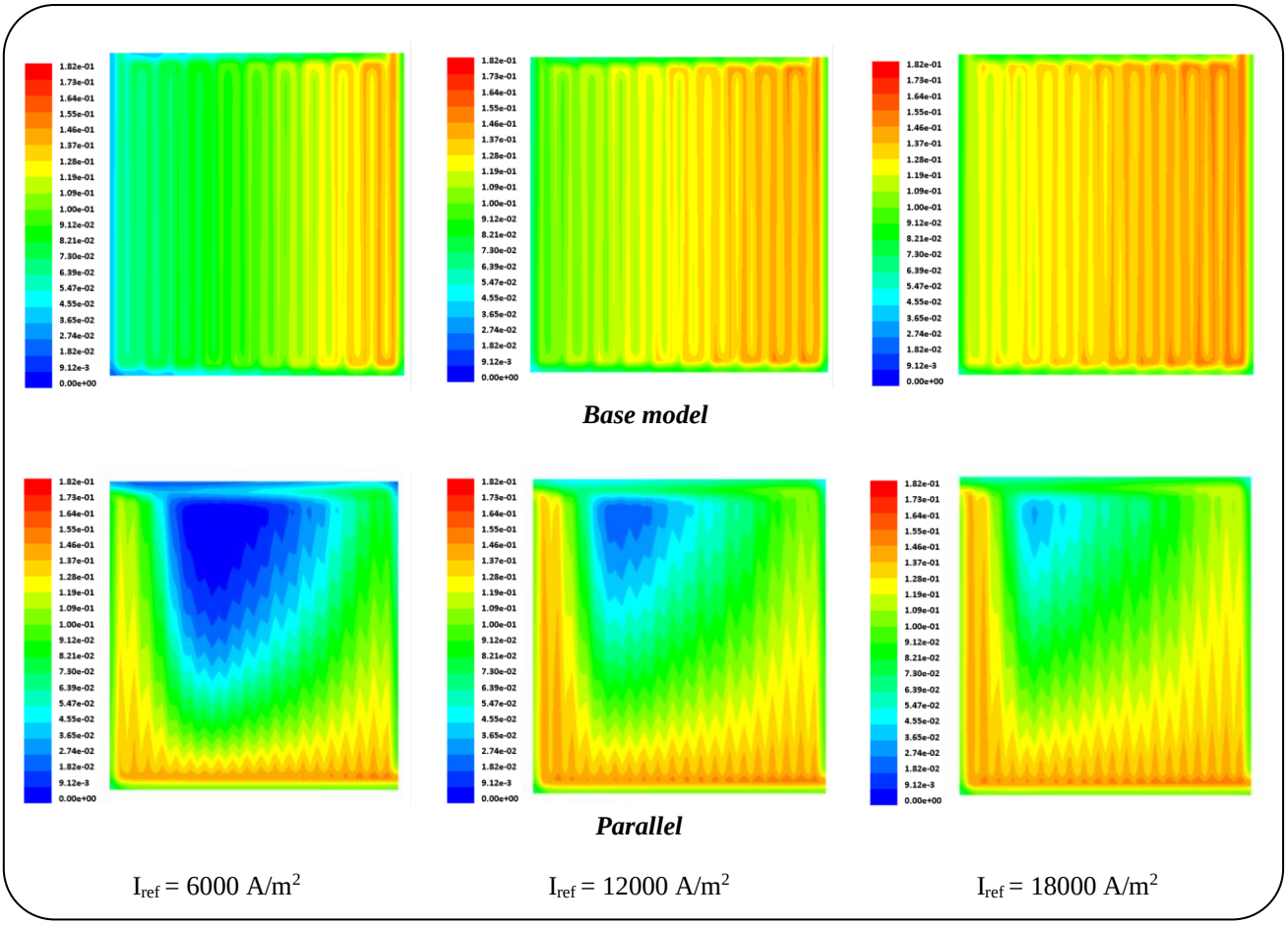

Fig. 14: Oxygen mass fraction contours on the cathode side (Catalyst Layer).

Fig. 21 depicts the flow velocity. The flow velocity increased as the reference current density increased.

Fig. 22 shows the temperature distribution of the flow field configuration in the catalyst layer on the cathodic side. As can be seen, the temperature declined from the inlet to the outlet in the parallel model due to water accumulation, preventing a uniform temperature distribution. In the base model, on the other hand, the temperature was uniformly distributed on the PEMFC.

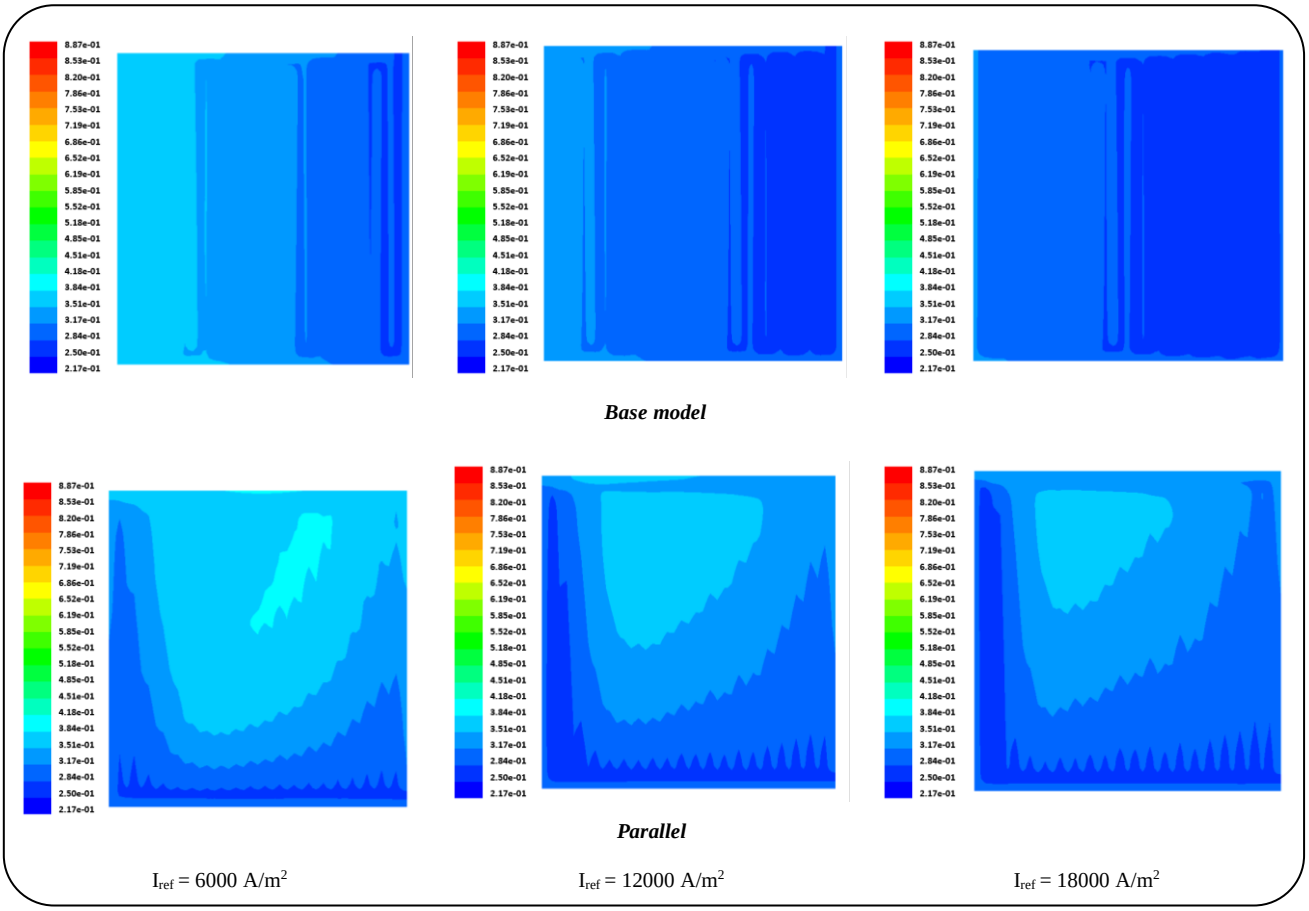

Fig. 15: Water mass fraction contours on the cathode side (Catalyst Layer).

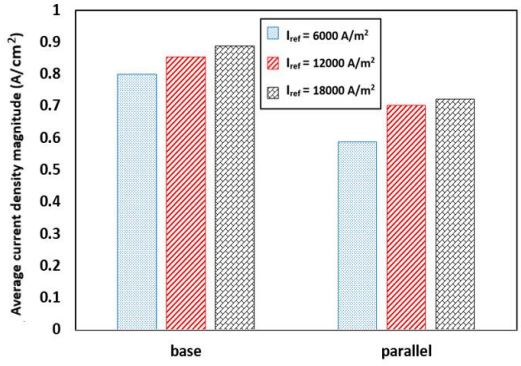

Fig. 16: Average current density distribution(A/cm^2).

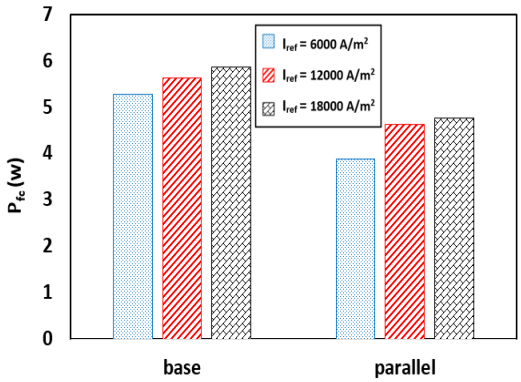

Fig. 17: Power generation for difference models (W).

The temperature in this type of fuel cell is uniform overall the stack and it is about 3 to 10 degrees rise in the intense reaction area, as can be seen in the figure. Also, the reference current density is one of the key criterion parameters that calculate the inlet concentration of the species and output current density. In other words, by increasing the reference current density the activity of the fuel cell is enhanced too and the temperature is raised in the fuel cell. The temperature especially on the cathode side has an important role in the performance of the PEMFC. If the temperature rises in the reaction area at the interface of the cathode catalyst and the membrane,

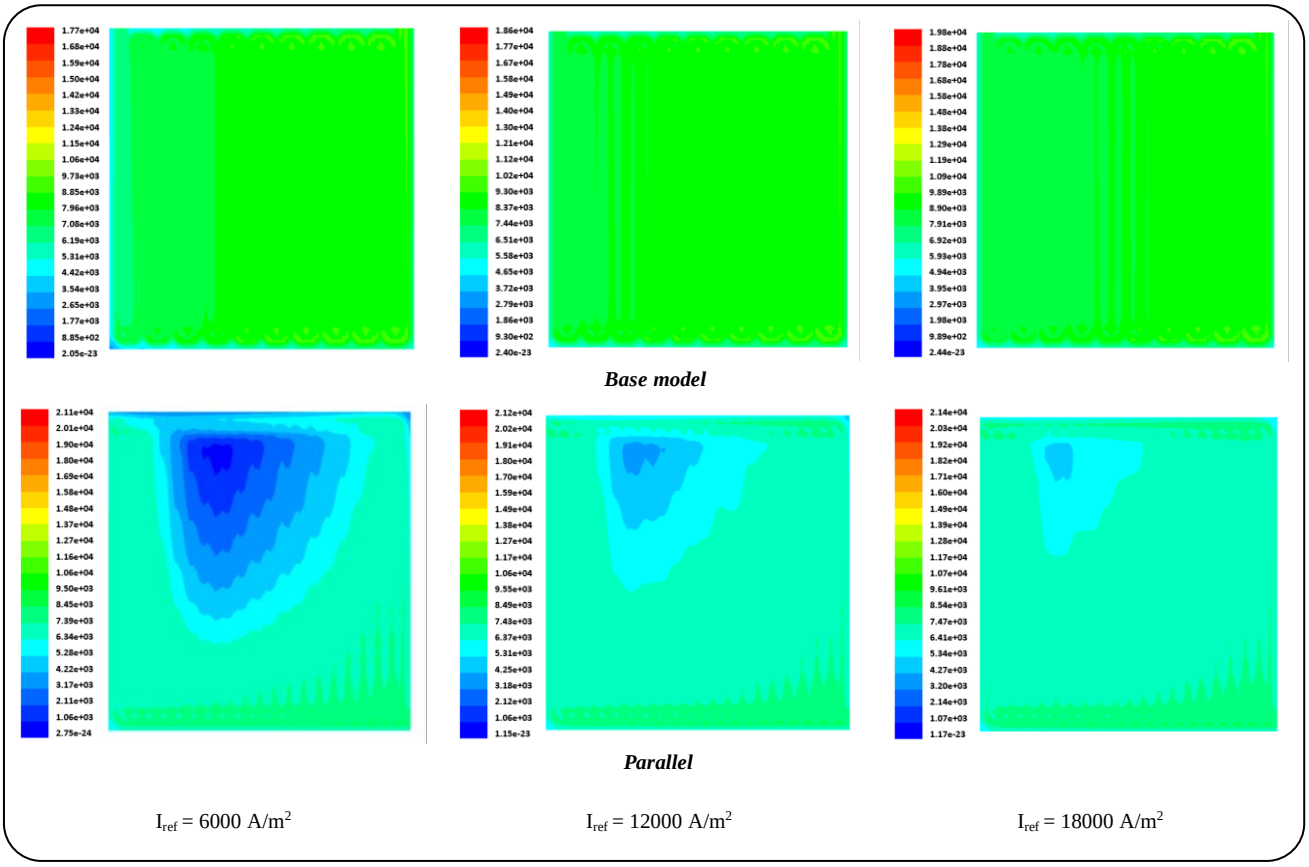

Fig. 18: Current density distribution for difference models (A/m^2).

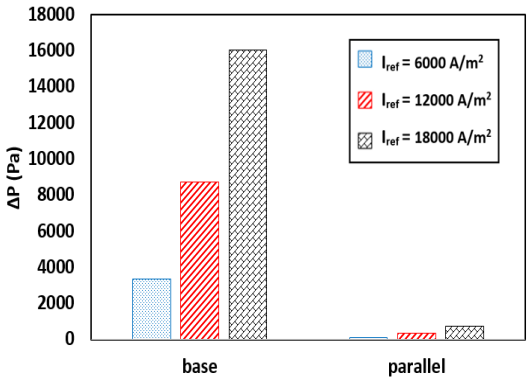

Fig. 19: Fuel cell pressure drop (Pa) for different models on the cathode channel.

it prevents to accumulation of water on the cathode side and prevents the water flooding phenomena. But, if the temperature is not controlled and exceeds the maximum desired value, it causes dehydration of the membrane which affects the performance of the membrane reversely. As can be seen, in the base model the temperature distribution is more uniform than the parallel model which improves the performance of the cell. Against, the parallel model, it is obvious that in the lower reference current density (6000), some regions of the reaction area have lesser temperature than the average of the cell. In this region, water accumulation can occur especially in the lower cell voltages.

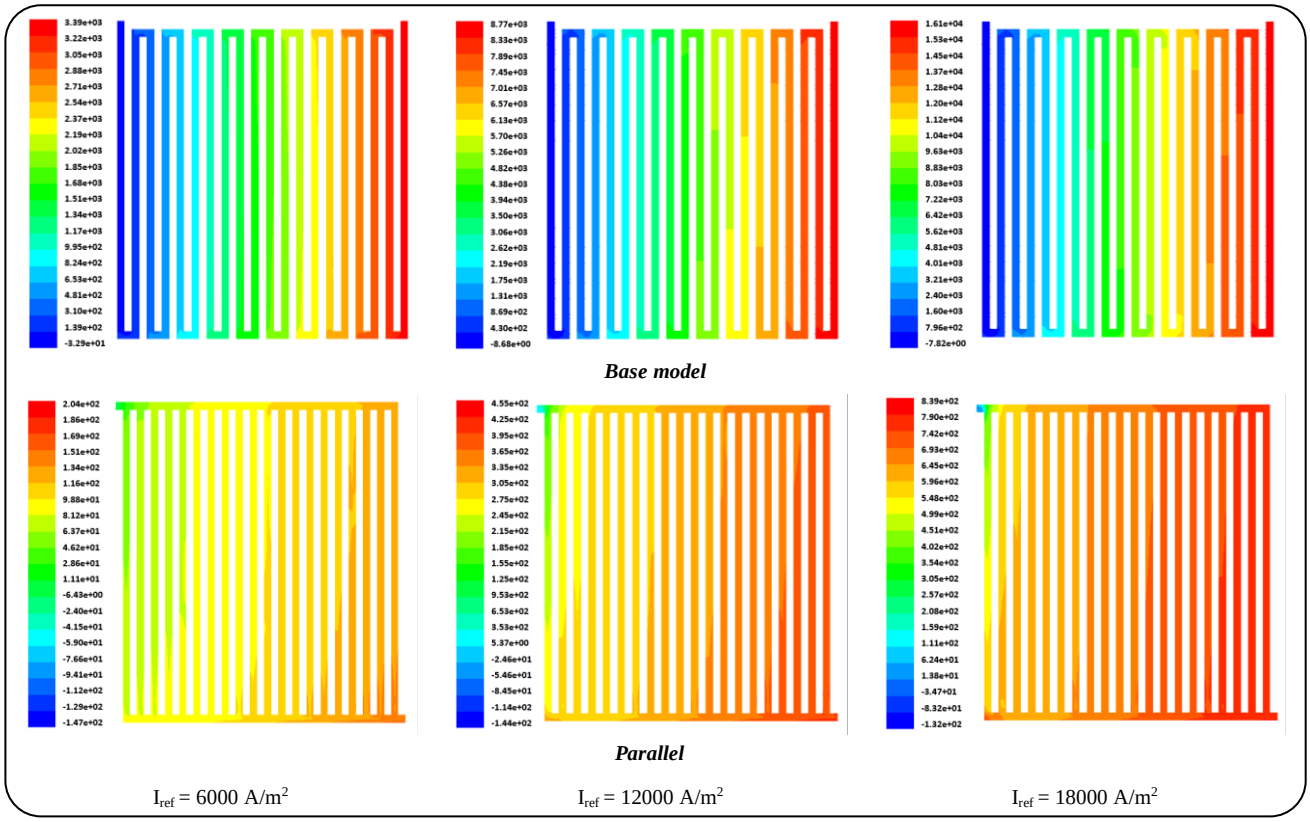

Fig. 20: Fuel cell pressure drop (Pa) contours for difference models on cathode channel.

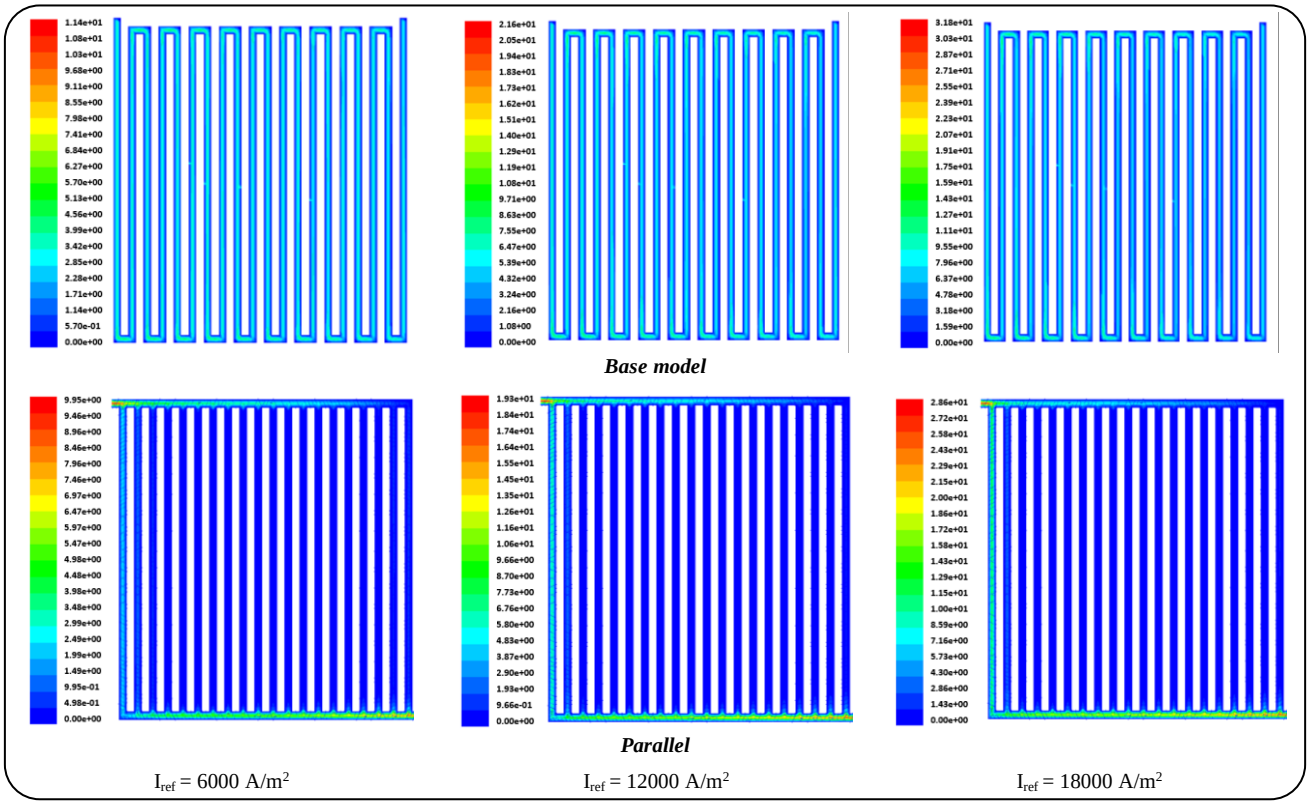

Fige. 21: Flow velocity contours (m/s) contours for difference models on the cathode channel.

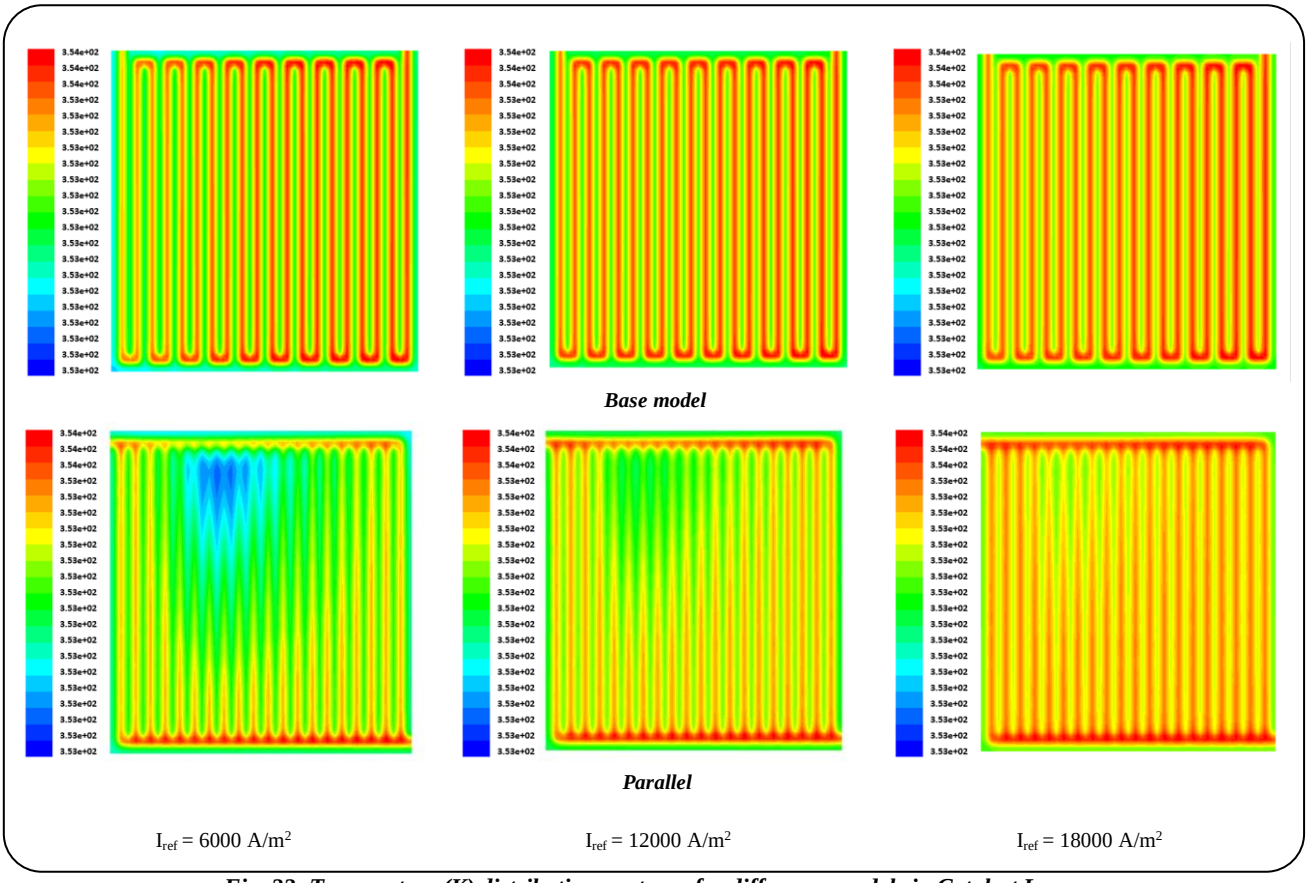

Fig. 22: Temperature (K) distribution contours for difference models in Catalyst Layer.

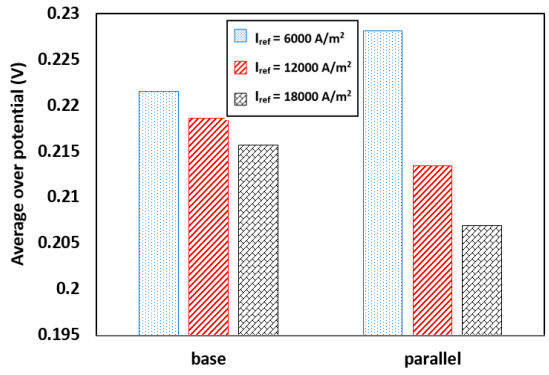

Fig. 23: Average overpotential (V).

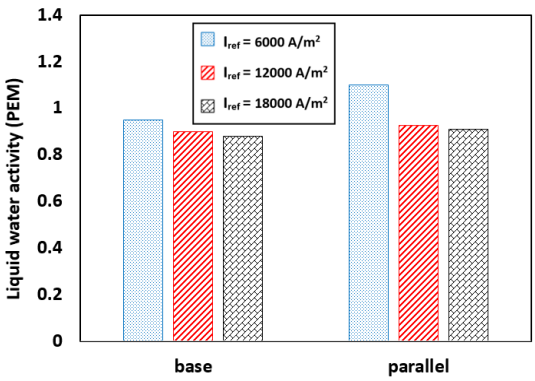

Fig. 24: Liquid water activity.

Furthermore, the average overpotential reduced as the reference current density increased (Fig.23). According to Fig. 24, liquid water production was lower at a larger current density. The parallel model had lower water production than the serpentine model. The maximum over potential in the parallel model for 6000 A/m^2 is 0.228 V.

CONCLUSIONS

PEMFC models with serpentine and parallel gas injection channels were designed and numerically simulated using CFD and FVM. The models were validated as the numerical results were in good agreement with earlier works. The simulation was performed at 0.6 V

for reference current densities of 6000, 12000, and 18000 A/m^2 to investigate the species distribution in the PEMFC, the pressure drop along the PEMFC, temperature and velocity distributions, current density, power density, liquid water production, and immersion. It was observed that the hydrogen and water concentrations decreased on the anode side, and water was produced on the cathode side due to reduced oxygen. The current density and output power were found to be higher in the serpentine model than in the parallel model due to a uniform current density on the serpentine PEMFC. The parallel model was observed to experience higher water accumulation, leading to immersion and PEMFC interruption. The parallel model underwent a lower pressure drop along the PEMFC and required lower additional power to pump the gases into the channels. The serpentine model had a more uniform temperature distribution. The distributions of the temperature, velocity and current density along the PEMFC were more uniform as higher reference current densities. The present study helps fuel cell designers and manufacturers exploit efficient and effective operating conditions and an optimal channel shape to enhance PEMFC performance.

Received : Jan. 11, 2022 ; Accepted : Apr. 4, 2022

REFERENCES

[1] Han Y., et al., Multisource Coordination Energy Management Strategy Based on SOC Consensus for a PEMFC–battery–supercapacitor Hybrid Tramway, *IEEE Transactions on Vehicular Technology*, **67(1)**: 296-305 (2017).

[2] Obayopo S.O., Bello-Ochende T., Meyer J.P., Three-Dimensional Optimisation of a Fuel Gas Channel of a Proton Exchange Membrane Fuel Cell for Maximum Current Density, *International Journal of Energy Research*, **37(3)**: 228-241 (2013).

[3] Pei P., Chen H., Main Factors Affecting the Lifetime of Proton Exchange Membrane Fuel Cells in Vehicle Applications: A Review, *Applied Energy*, **125**: 60-75 (2014).

[4] Wu H.-W., A Review of Recent Development: Transport And Performance Modeling of PEM Fuel Cells, *Applied Energy*, **165**: 81-106 (2016).

[5] Pourmahmoud N., et al., Three-Dimensional Numerical Analysis of Proton Exchange Membrane Fuel Cell, *Journal of Mechanical Science and Technology*, **25(10)**: 2665 (2011).

[6] Wang Y., et al., Materials, Technological Status, and Fundamentals of PEM Fuel Cells–A Review, *Materials Today*, **32**: 178-203 (2020).

[7] Chen H., et al., Influencing Sensitivities of Critical Operating Parameters on PEMFC Output Performance and Gas Distribution Quality Under Different Electrical Load Conditions, *Applied Energy*, **255**: 113849 (2019).

[8] Wang L., et al., A parametric Study of PEM Fuel Cell Performances, *International Journal of Hydrogen Energy*, **28(11)**: 1263-1272 (2003).

[9] Santarelli M., Torchio M., Experimental Analysis of the Effects of the Operating Variables on the Performance of a Single PEMFC, *Energy Conversion and Management*, **48(1)**: 40-51 (2007).

[10] Yang Y., et al., Overall and Local Effects of Operating Conditions in PEM Fuel Cells with Dead-Ended Anode, *International Journal of Hydrogen Energy*, **42(7)**: 4690-4698 (2017).

[11] Kim D.K., et al., Experimental and Computational Study on the Dynamic Interaction Between Load Variation and Back Pressure Control in a Polymer Electrolyte Membrane Fuel Cell for Automotive Application, *International Journal of Hydrogen Energy*, **40(36)**: 12370-12381 (2015).

[12] Kadjo A.-J., et al., Improvement of Proton Exchange Membrane Fuel Cell Electrical Performance by Optimization of Operating Parameters and Electrodes Preparation, *Journal of Power Sources*, **172(2)**: 613-622 (2007).

[13] Kahveci E.E., Taymaz I., Assessment of Single-Serpentine PEM Fuel Cell Model Developed by Computational Fluid Dynamics, *Fuel*, **217**: 51-58 (2018).

[14] Zeroual M., et al., Numerical Study of The Effect of the Inlet Pressure and the Height of Gas Channel on the Distribution and Consumption of Reagents in a Fuel Cell (PEMFC). *Energy procedia*, **18**: 205-214 (2012).

[15] Kim H.-Y., Kim K., Numerical Study on the Effects of Gas Humidity on Proton-Exchange Membrane Fuel Cell Performance, *International Journal of Hydrogen Energy*, **41(27)**: 11776-11783 (2016).

[16] Zhang Q., et al., Experimental Study of Variable Operating Parameters Effects on Overall PEMFC Performance And Spatial Performance Distribution, *Energy*, **115**: 550-560 (2016).

[17] Chavan S.L., Talange D.B., Modeling and Performance Evaluation of PEM Fuel Cell by Controlling Its Input Parameters, *Energy*, **138**: 437-445 (2017).

[18] Wang B., et al., Numerical Analysis of Operating Conditions Effects on PEMFC with Anode Recirculation,*Energy*, **173**: 844-856 (2019).

[19] Guvelioglu G.H., Stenger H.G., Flow Rate and Humidification Effects on a PEM Fuel Cell Performance and Operation, *Journal of Power Sources*, **163(2)**: 882-891 (2007).

[20] Gomez A., et al., Effect of Operating Parameters on the Transient Performance of a Polymer Electrolyte Membrane Fuel Cell Stack with a Dead-End Anode, *Applied Energy*, **130**: 692-701 (2014).

[21] Boulon L., et al. "Energy Management of a Fuel Cell System: Influence of the Air Supply Control on the Water Issues", *in 2010 IEEE International Symposium on Industrial Electronics*. (2010). IEEE.

[22] Wasterlain S., et al., Study of Temperature, Air Dew Point Temperature and Reactant Flow Effects on Proton Exchange Membrane Fuel Cell Performances Using Electrochemical Spectroscopy and Voltammetry Techniques, *Journal of Power Sources*, **195(4)**: 984-993 (2010).

[23] Ahmadi N., Rezazadeh S., Mirzaee I., Study the Effect of Various Operating Parameters of Proton Exchange Membrane, *Periodica Polytechnica Chemical Engineering*, **59(3)**: 221-235 (2015).

[24] Ahmadi N., Ahmadpour V., Rezazadeh S., Numerical Investigation of Species Distribution and the Anode Transfer Coefficient Effect on the Proton Exchange Membrane Fuel Cell (PEMFC) Performance, *Heat Transfer Research*, **46(10)**: 881-901 (2015).

[25] Ahmadi N., et al., Three-Dimensional Computational Fluid Dynamic Study on Performance of Polymer Exchange Membrane Fuel Cell (PEMFC) in Different Cell Potential, *Iranian Journal of Science and Technology. Transactions of Mechanical Engineering*, **36(M2)**: 129 (2012).

[26] Ahmed D.H., Sung H.J., Effects of Channel Geometrical Configuration and Shoulder Width on PEMFC Performance at High Current Density, *Journal of Power Sources*, **162(1)**: 327-339 (2006).

[27] Jabbary A., et al., Numerical Investigation of 3D Rhombus Designed PEMFC on the Cell Performance, *International Journal of Green Energy*, **18(5)**: 425-442 (2021).

[28] Jeon D., et al., The Effect of Serpentine Flow-Field Designs on PEM Fuel Cell Performance, *International Journal of Hydrogen Energy*, **33(3)**: 1052-1066 (2008).

[29] Min C., et al., A Comprehensive Analysis of Secondary Flow Effects on the Performance of PEMFCs with Modified Serpentine Flow Fields, *Energy Conversion and Management*, **180**: 1217-1224 (2019).

[30] Rezazadeh S., Ahmadi N., Ahmadi, Numerical Investigation of Gas Channel Shape Effect on Proton Exchange Membrane Fuel Cell Performance, *Journal of the Brazilian Society of Mechanical Sciences and Engineering*, **37(3)**: 789-802 (2015).

[31] Özdemir, S.N., Taymaz İ., CFD Investigation of Different Flow Field Designs for Efficient PEMFC Performance, *Sakarya University Journal of Science*, **25(3)**: 690-698 (2021).

[32] Samanipour H., et al., The Study of Cylindrical Polymer Fuel Cell's Performance and the Investigation of Gradual Geometry Changes' Effect on Its Performance, *Periodica Polytechnica Chemical Engineering*, **63(3)**: 513-526 (2019).

[33] Mohammedi A., Sahli Y., Moussa H.B., 3D Investigation of the Channel Cross-Section Configuration Effect on the Power Delivered by PEMFCs with Straight Channels, *Fuel*, **263**: 116713 (2020).

[34] Sadeghi H., et al., Numerical Investigation of Gas Channel Geometry of Proton Exchange Membrane Fuel Cell, *Renewable Energy Research and Application*, **1(1)**: 93-114 (2020).

[35] Sheikhmohamadi A., et al., The Effect of Novel Designs on the Performance of Polymer Electrolyte Membrane Fuel Cell, *AUT Journal of Mechanical Engineering*,**4(3)**: 331-346 (2020).

[36] Chippar P., Ju H., Numerical Modeling and Investigation of Gas Crossover Effects In High Temperature Proton Exchange Membrane (PEM) Fuel Cells, *International Journal of Hydrogen Energy*, **38(18)**: 7704-7714 (2013).

[37] Patankar S.V., "Numerical Heat Transfer and Fluid Flow". (2018): CRC Press.

[38] Sheikh Mohammadi A., et al., Influence of Gas Channels and Gas Diffusion Layers Configuration on the Performance of Polymer Electrolyte Membrane Fuel Cell, *Journal of Solid and Fluid Mechanics*, **9(3)**: 249-263 (2019).